



Discover Generics

Cost-Effective CT & MRI Contrast Agents



**FRESENIUS
KABI**

[WATCH VIDEO](#)

AJNR

Comparison of Image Quality and Radiation Dose in Pediatric Temporal Bone CT Using Photon-Counting Detector CT and Energy-Integrating Detector CT

Jeong Sub Lee, John Kim, Jayapalli R. Bapuraj and Ashok Srinivasan

This information is current as of June 22, 2025.

AJNR Am J Neuroradiol 2024, 45 (9) 1322-1326

doi: <https://doi.org/10.3174/ajnr.A8276>

<http://www.ajnr.org/content/45/9/1322>

Comparison of Image Quality and Radiation Dose in Pediatric Temporal Bone CT Using Photon-Counting Detector CT and Energy-Integrating Detector CT

Jeong Sub Lee, John Kim, Jayapalli R. Bapuraj, and Ashok Srinivasan

ABSTRACT

BACKGROUND AND PURPOSE: Currently, there is a lack of research directly comparing photon-counting detector CT (PCD-CT) and energy-integrating detector CT (EID-CT) in pediatric temporal bone CT imaging. The purpose of this study was to compare the image quality and radiation dose of temporal bone CT scans in pediatric patients acquired with PCD-CT and EID-CT.

MATERIALS AND METHODS: The retrospective study included a total of 110 pediatric temporal bone CT scans (PCD-CT, $n = 52$; EID-CT, $n = 58$). Two independent readers evaluated the spatial resolution of 4 anatomic structures (tympanic membrane, incudostapedial joint, stapedial crura, and cochlear modiolus) and overall image quality by using a 4-point scale. Interreader agreement was assessed. Dose-length product for each CT was compared, and subgroup analyses were performed based on age (younger than 3 years, 3–5 years, 6–11 years, and 12 years and above).

RESULTS: PCD-CT demonstrated statistically significantly higher scores than EID-CT for all items (tympanic membrane, 2.9 versus 2.4; incudostapedial joint, 3.6 versus 2.6; stapedial crura, 3.2 versus 2.4; cochlear modiolus, 3.4 versus 2.8; overall image quality, 3.6 versus 2.8; $P < .05$). Interreader agreement ranged from good to excellent (interclass correlation coefficients, 0.6–0.81). PCD-CT exhibited a 43% dose reduction compared with EID-CT, with a particularly substantial reduction of over 70% in the subgroups of children younger than 6 years.

CONCLUSIONS: PCD temporal bone CT achieves significantly superior imaging quality at a lower radiation dose compared with EID-CT.

ABBREVIATIONS: AEC = automatic exposure control; DLP = dose-length product; EID-CT = energy-integrating detector CT; ICC = interclass correlation coefficient; PCD-CT = photon-counting detector CT

A high spatial resolution image is necessary for distinguishing small internal structures in temporal bone CT.^{1,2} However, the need to obtain high-resolution images should be balanced with the need to limit radiation dose, especially in pediatric patients.

Conventional energy-integrating detector CT (EID-CT) utilizes a scintillator layer to convert x-rays into visible light, and then a photodiode converts it back into an electric signal. This process requires septa, which hinders maximal achievable spatial resolution.^{3–5}

Photon-counting detector CT (PCD-CT) is the most recently commercialized CT technology. In contrast to EID-CT, PCD-CT differs in that it utilizes semiconductor detector materials without a scintillator layer to convert x-rays into electronic signals.^{6–8} A PCD can measure the number and energy of x-ray photons and is not dependent on energy-weighting. Thus, lower energy x-ray

thresholds can be selected to improve iodine or soft tissue contrast.^{5,7,9,10} Additionally, material decomposition can be achieved with a single x-ray tube and various reconstructions such as virtual noncontrast and virtual monochromatic images can also be created. Unlike EID-CT, it lacks detector septa, enabling image acquisition with a smaller pixel size and better spatial resolution. The removal of electronic noise also allows for the application of ultra-low-dose CT protocols, presenting an advantage.^{5,11}

Prior temporal bone imaging studies in cadaveric models and adult patients have shown reduced radiation dose and superior spatial resolution with PCD-CT compared with EID-CT. However, there is currently no comparative study specifically focused on pediatric patients.^{3,12–15}

Therefore, the aim of this study is to compare the image quality and radiation dose of pediatric temporal bone CT obtained with PCD-CT and EID-CT.

MATERIALS AND METHODS

Patients

This retrospective study received approval from our institutional review board (IRB No. 00244315), and informed consent was

Received February 5, 2024; accepted after revision March 26.

From the Department of Radiology (J.S.L.), Jeju National University Hospital, Jeju National University College of Medicine, Jeju-si, Jeju-do, Republic of Korea and Department of Radiology (J.K., J.R.B., A.S.), University of Michigan, Ann Arbor, Michigan.

Please address correspondence to John Kim, MD, 1500 E. Medical Center Dr., B2A205A, Ann Arbor, MI, 48109-5030; e-mail: johank@med.umich.edu

<http://dx.doi.org/10.3174/ajnr.A8276>

SUMMARY

PREVIOUS LITERATURE: According to previous studies by using adult or cadaveric models, PCD-CT can obtain images of better quality compared with EID-CT due to the characteristics of the detector, and can also reduce radiation dose. However, there is currently a lack of research directly comparing PCD-CT and EID-CT in pediatric temporal bone CT imaging.

KEY FINDINGS: PCD-CT exhibited significantly better subjective spatial resolution and overall image quality compared with EID-CT ($P < .05$). The radiation dose was reduced by 43.3% with PCD-CT compared with EID-CT, with more than 70% reduction observed in subgroups aged younger than 6 years.

KNOWLEDGE ADVANCEMENT: In pediatric temporal bone CT, PCD-CT can obtain better images with less radiation dose. This will be of great benefit in the diagnostic imaging of pediatric patients.

waived. The study included 61 consecutive pediatric patients younger than 18 years old who underwent temporal bone CT scans from April 2023 to November 2023 by using PCD-CT (Naeotom Alpha; Siemens Healthineers), as well as 64 consecutive pediatric patients who underwent temporal bone imaging from September 2022 to March 2023 by using conventional EID-CT (Discovery HD750; GE Healthcare).

CT Protocol

Table 1 shows the scan parameters for both CT scanners. For PCD-CT, to adjust radiation dose, protocols were varied based on a 6-year-old reference and all scans were conducted in high-resolution mode. Automatic exposure control (AEC) software, including CARE Dose 4D and CARE kV were used. For EID-CT, scan parameters were adjusted for 3 groups: those younger than 3 years old, those between 3 and 11 years old, and those 12 years of age and older, with all scans performed in high-resolution mode. Fixed mA was used instead of using AEC software.

Image Review

All images were reconstructed into axial, coronal, and sagittal planes. Two board-certified radiologists with 5 (J.S.L.) and 14 (J.K.) years of temporal bone imaging experience independently and blindly reviewed the images of PCD-CT and EID-CT by using a PACS. Subjective spatial resolution and image quality was assessed for 4 anatomic structures (tympanic membrane, incudostapedial joint, stapedial crura, and cochlear modiolus)

by using a 4-point Likert scale: 1 = inferior resolution with degraded visualization; 2 = slightly inferior resolution without affecting visualization; 3 = slightly superior resolution without affecting visualization; and 4 = superior resolution with improved visualization (Fig 1). The assessment of structures was conducted by selecting the best visualized or most normal side of the temporal bone CT. After all the patients had been evaluated and scored, for structures that were deemed unassessable (eg, fluid in the middle cavity obscuring the tympanic membrane), consensus was reached by both observers for their exclusion. Unassessable structures were excluded while unaffected remaining structures were included. Additionally, overall image quality was evaluated by using a 4-point Likert scale: 1 = poor image quality with degraded diagnostic performance; 2 = fair image quality without degraded diagnostic performance; 3 = good image quality without remarkable image quality disturbance; and 4 = excellent image quality without image quality disturbance.

Radiation Dose

Radiologist J.S.L. extracted the radiation dose details from the dose reports of individual patients who had already been included on the PACS as part of their imaging records and compared the dose-length product (DLP) between the 2 groups. Because protocol adjustments for radiation dose reduction were based on different age ranges for the 2 CT scanners, we divided the study population into 4 subgroups (younger than 3 years, 3–5 years,

Table 1: Scan parameters for PCD-CT and EID-CT

	PCD-CT		EID-CT		
	<6 yr	≥6 yr	<3 yr	3–11 yr	≥12 yr
Tube voltage (kVp)	90 (ref)	120 (ref)	120	120	120
Tube current	58 mAs (quality ref)	99 mAs (quality ref)	100 mA	120 mA	150 mA
Image quality metrics	IQ 42	IQ 110	—	—	—
Matrix size	768 × 768	768 × 768	512 × 512	512 × 512	512 × 512
Pitch	0.85	0.85	0.531	0.531	0.531
Gantry rotation time	0.5	0.5	0.5	0.5	0.5
Collimation	120 × 0.2 mm	120 × 0.2 mm	64 × 0.675 mm	64 × 0.675 mm	64 × 0.675 mm
Kernel	Hr72	Hr72	HD bone	HD bone	HD bone
Iterative reconstruction	QIR off	QIR off	ASiR 30%	ASiR 30%	ASiR 30%
Slice thickness	0.3 mm	0.3 mm	0.625 mm	0.625 mm	0.625 mm
Interval	0.3 mm	0.3 mm	0.312 mm	0.312 mm	0.312 mm
Automatic exposure control	Used	Used	None	None	None

Note:—QIR indicates Quantum Iterative Reconstruction; Ref, reference; ASiR, Adaptive Statistical Iterative Reconstruction; IQ, image quality; Hr, head regular; HD, high definition.

6–11 years, and 12 years and older) and compared the average DLP within each subgroup.

Statistical Analysis

Age, weight, DLP, and Likert scales for quality analysis were compared by using mean values for each CT group, with the statistical significance of these variables determined through *t* test. In subgroup analyses, as the values did not adhere to a normal distribution, the Mann-Whitney U test was used. Sex distribution between the 2 patient groups was assessed by using a χ^2 test. To assess the interreader agreement, the intraclass correlation coefficient (ICC) was used. The agreement was categorized as poor (<0.40), fair (0.40 – 0.59), good (0.60 – 0.75), and excellent (>0.75). A *P* value $< .05$ was considered statistically significant. The statistical analysis was conducted by using SPSS version 20 (IBM).

RESULTS

Among the 125 enrolled patients, 12 patients (PCD-CT, *n* = 6; EID-CT, *n* = 6) who were imaged by using only a contrast-enhanced protocol without precontrast images, and 3 patients (PCD-CT) who did not have high-resolution temporal bone images were excluded from the study. A total of 110 patients were included (PCD-CT, *n* = 52; EID-CT, *n* = 58), with reasons for examination being hearing loss (*n* = 65), inflammation or infection (*n* = 26), congenital malformation (*n* = 9), and

miscellaneous reasons (ie, mass, trauma, hyperacusis, dizziness, etc; *n* = 10). Patient characteristics are presented in Table 2. There were no statistically significant differences in the mean age, sex distribution, and weight between PCD-CT and EID-CT groups (*P* $> .05$). Within the subgroups divided by age, there were no statistically significant differences in mean weight of the populations between the 2 CT groups (*P* $> .05$).

Table 3 shows subjective spatial resolution and image quality scores for the 4 anatomic structures and overall image quality. PCD-CT exhibited significantly higher scores than EID-CT for all assessed items (*P* $< .05$, Fig 2). PCD-CT exhibited values exceeding a mean of 3.0 for all items except the tympanic membrane, whereas EID-CT scored below a mean of 3.0 for all items. In the tympanic membrane, both CT scans exhibited the lowest scores, with the mean difference being relatively the smallest (2.9 ± 1.1 versus 2.4 ± 0.7 , *P* = .022). The highest-scoring items were the incudostapedial joint and overall image quality for PCD-CT, and the average score difference between these items for the 2 CT scans was relatively large (3.6 ± 0.7 versus 2.6 ± 0.5 , 3.6 ± 0.6 versus 2.8 ± 0.3 , *P* $< .001$, respectively). The interreader agreement for spatial resolution scores for each item indicated good or excellent agreement in both CT scans (ICCs, 0.6 – 0.81 , Table 4).

Table 5 shows DLP for both CT scans. The mean DLP (mGy \times cm) showed significantly lower values on PCD-CT compared with EID-CT (91.3 ± 57.1 versus 161.0 ± 35.9 , *P* $< .001$). When comparing age-related subgroups, PCD-CT

consistently demonstrated lower mean values across all age subgroups (*P* $< .01$, Fig 3). In the overall group, PCD-CT exhibited a dose reduction of approximately 43% compared with EID-CT. Particularly, PCD-CT exhibited a significantly substantial dose reduction (72%–77%) compared with EID-CT in the age groups younger than 6 years old.

DISCUSSION

In this study, PCD-CT demonstrated superior subjective spatial resolution and image quality in pediatric temporal bone imaging compared with EID-CT, with an additional advantage of lower radiation dose. This study demonstrated

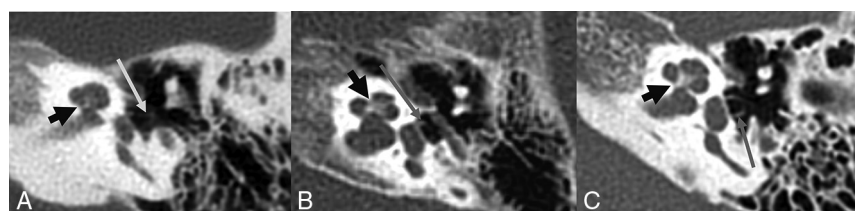


FIG 1. Likert scale examples of subjective spatial resolution for different patients (A, EID-CT; B and C, PCD-CT). The stapedial crus (long arrow) and cochlear modiolus (short arrow) are rated as 2 points in (A), 3 points in (B), and 4 points in (C), respectively.

Table 2: Patient characteristics on PCD-CT and EID-CT^a

	PCD-CT (<i>n</i> = 52)	EID-CT (<i>n</i> = 58)	<i>P</i> Value
Age (yr)	6.2 ± 4.3	6.9 ± 5.5	.466
Sex (male/female)	24/28	31/27	.445
Weight (kg)	29.0 ± 22.1	30.6 ± 24.0	.705

^a Data, excluding sex, are presented as mean \pm standard deviation. Statistical significance is set at *P* $< .05$.

Table 3: Subjective spatial resolution and image quality scores of PCD-CT and EID-CT^a

	Tympanic Membrane	Incudostapedial Joint	Stapedial Crura	Cochlear Modiolus	Overall Image Quality
Reader 1 PCD-CT	2.9 ± 0.9	3.7 ± 0.6	3.1 ± 0.8	3.7 ± 0.8	3.6 ± 0.7
EID-CT	2.4 ± 0.7	2.5 ± 0.6	2.2 ± 0.6	2.8 ± 0.5	2.8 ± 0.4
<i>P</i> value	.001	$< .001$	$< .001$	$< .001$	$< .001$
Reader 2 PCD-CT	3.4 ± 0.6	3.7 ± 0.6	3.4 ± 0.7	3.8 ± 0.4	3.7 ± 0.6
EID-CT	2.7 ± 0.6	2.8 ± 0.5	2.6 ± 0.7	3.0 ± 0.4	2.9 ± 0.3
<i>P</i> value	$< .001$	$< .001$	$< .001$	$< .001$	$< .001$
Mean PCD-CT	2.9 ± 1.1	3.6 ± 0.7	3.2 ± 0.8	3.4 ± 1.1	3.6 ± 0.6
EID-CT	2.4 ± 0.7	2.6 ± 0.5	2.4 ± 0.6	2.8 ± 0.6	2.8 ± 0.3
<i>P</i> value	.022	$< .001$	$< .001$	$< .001$	$< .001$

^a Data are presented as mean \pm standard deviation. Statistical significance is set at *P* $< .05$.

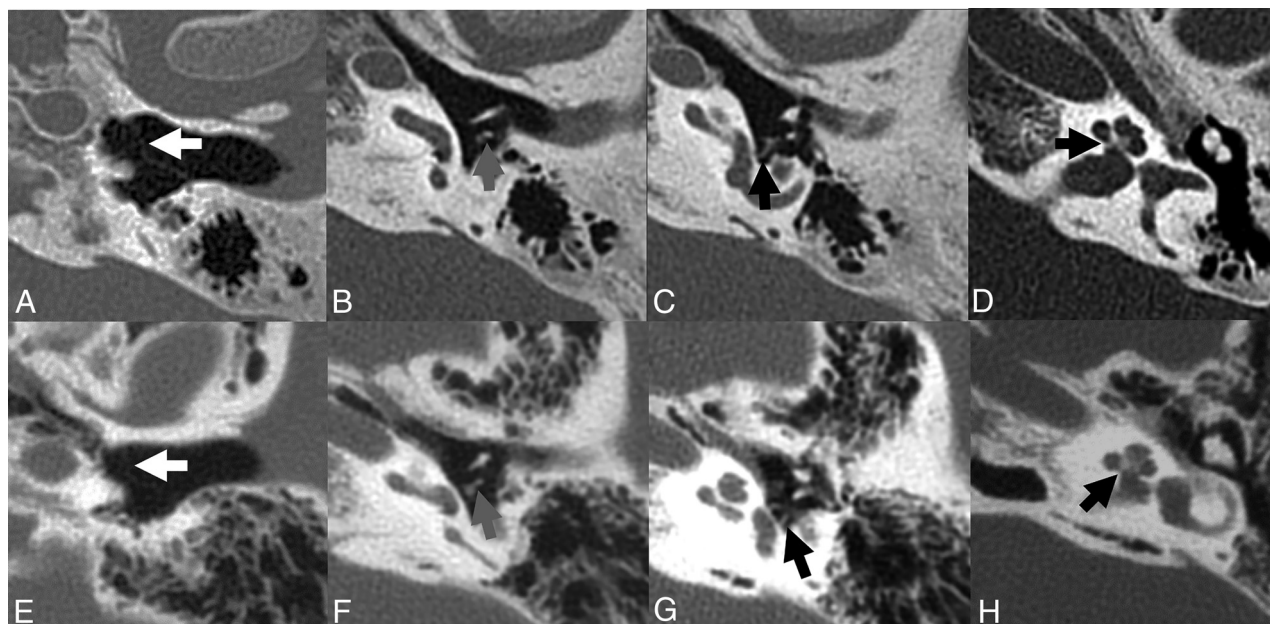


FIG 2. A–D, Left temporal bone CT images of a 14-year-old adolescent boy from PCD-CT. The axial CT images show anatomic structures, including the tympanic membrane (A, arrow), incudostapedial joint (B, arrow), stapedial crus (C, arrow), and cochlear modiolus (D, arrow). Both readers rated a score of 4 for all anatomic structures and overall image quality. E–H, Left temporal bone CT images of a 13-year-old adolescent girl from EID-CT. The axial CT images show anatomic structures, including the tympanic membrane (E, arrow), incudostapedial joint (F, arrow), stapedial crus (G, arrow), and cochlear modiolus (H, arrow). Both readers rated a score of 3 for incudostapedial joint, cochlear modiolus, and overall image quality. The tympanic membrane and stapedial crura were rated a score of 2 and 4, respectively.

Table 4: Interreader agreement with ICC for subjective spatial resolution scores

	PCD-CT		EID-CT	
	ICC (2,1)	95% CI	ICC (2,1)	95% CI
Tympanic membrane	0.631	0.223–0.812	0.661	0.358–0.813
Incudostapedial joint	0.773	0.602–0.870	0.630	0.309–0.794
Stapedial crura	0.664	0.401–0.810	0.640	0.265–0.810
Cochlear modiolus	0.630	0.344–0.792	0.634	0.381–0.784
Overall image quality	0.808	0.667–0.890	0.632	0.379–0.782

Table 5: Dose length products (mGy x cm) of PCD-CT and EID-CT^a

Age (yr)	PCD-CT (n = 52)	EID-CT (n = 58)	P Value	Reduction Rate
All	91.3 ± 57.1	161.0 ± 35.9	<.001	43.3%
<3	27.8 ± 8.4 (n=13)	119.9 ± 15.9 (n=6)	<.001	76.8%
3–5	44.2 ± 9.7 (n=10)	159.4 ± 16.9 (n=11)	<.001	72.3%
6–11	129.3 ± 3.0 (n=23)	163.5 ± 10.3 (n=14)	<.001	20.9%
≥12	161.2 ± 20.1 (n=6)	198.6 ± 29.6 (n=17)	.006	18.8%

^a Data are presented as mean ± standard deviation. Statistical significance is set at $P < .05$.

consistent results with previous studies, supporting the notion that PCD-CT provides better image quality and high-resolution images compared with conventional EID-CT. The ability of PCD-CT to achieve thinner slice thickness is considered to be one of the primary factors contributing to this.¹²

The tympanic membrane, being a thin structure challenging to visualize distinctly in CT, scored the lowest in both CT scans. However, in PCD-CT, it presented a relatively improved subjective spatial resolution with an average score close to 3.0 (slightly superior resolution without affecting visualization). While EID-CT yielded scores below a mean of 3.0 for all items (2.4–2.8), PCD-CT showed values exceeding a mean of 3.5 for most items, indicating improved resolution. In previously published studies,

spatial resolution scores evaluated for anatomic structures were significantly higher in PCD-CT, and image quality scores were also superior.^{3,13,15}

Regarding radiation dose, PCD-CT demonstrates a significant reduction compared with EID-CT in pediatric temporal bone imaging. Benson et al³ reported a 31% dose reduction in a study involving 13 adult patients, and Hermans et al¹³ showed a 26% dose reduction in a study with 36 adults. In this study, in which a protocol identical to that used for adults was applied to subgroups aged 6 years and older, PCD-CT exhibited a dose reduction of approximately 20%, similar to previous studies. Particularly, in the subgroup

younger than 6 years, where the dose was set even lower in PCD-CT, a dose reduction of more than 70% compared with EID-CT was achievable. The radiation sensitivity is greater in children than in adults, increasing with younger age.¹⁶ Therefore, the significance of this study lies in demonstrating the advantage of PCD-CT, which can obtain superior image quality and spatial resolution with significantly lower radiation doses, especially in young pediatric patients.

This study has the following limitations. First, it used a retrospective study design with a small sample size. However, to our knowledge, this is the first dedicated pediatric and largest cohort of temporal bone CT evaluations to date described in the literature. Second, although the radiologists were blinded to the type

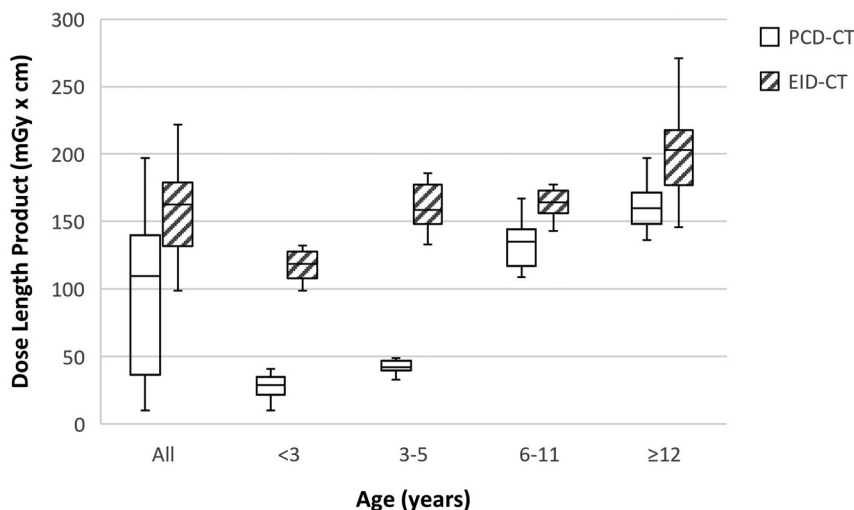


FIG 3. Boxplot graphs for the dose-length products of photon-counting detector CT and energy-integrating detector CT in age-related subgroups.

of images, the superior and sharper appearing PCD-CT may be a giveaway and cannot be concealed by any imaging subterfuge. Third, this study focused on only normal structures. However, the notable resolution improvement of PCD-CT suggests its potential utility in observing small structures in pediatric patients for the assessment of pathology or anatomic anomalies. Furthermore, the image evaluations were compared by using subjective assessment techniques, and it should be noted that different age-based dose-reduction protocols were applied for the 2 CT scans. In an ideal situation, a prospective randomized study comparing the 2 CT modalities would be the preferred design, including quantitative analysis, and the authors hope that this endeavor would be the first step in recognizing the superiority of PCD-CT.

CONCLUSIONS

PCD-CT can significantly reduce radiation dose while providing superior spatial resolution and image quality in pediatric temporal bone CT, making it a valuable imaging asset for the management of pediatric patients.

Disclosure forms provided by the authors are available with the full text and PDF of this article at www.ajnr.org.

REFERENCES

1. Lane JI, Lindell EP, Witte RJ, et al. Middle and inner ear: improved depiction with multiplanar reconstruction of volumetric CT data. *Radiographics* 2006;26:115–24 [CrossRef](#)
2. Leng S, Diehn FE, Lane JI, et al. Temporal bone CT: improved image quality and potential for decreased radiation dose using an

ultra-high-resolution scan mode with an iterative reconstruction algorithm. *AJNR Am J Neuroradiol* 2015;36:1599–603 [CrossRef](#)

3. Benson JC, Rajendran K, Lane JI, et al. A new frontier in temporal bone imaging: photon-counting detector CT demonstrates superior visualization of critical anatomic structures at reduced radiation dose. *AJNR Am J Neuroradiol* 2022;43:579–84 [CrossRef](#)
4. Flohr T, Petersilka M, Henning A, et al. Photon-counting CT review. *Phys Med* 2020;79:126–36 [CrossRef](#)
5. Esquivel A, Ferrero A, Mileto A, et al. Photon-counting detector CT: key points radiologists should know. *Korean J Radiology* 2022;23:854–65 [CrossRef](#)
6. Rajendran K, Petersilka M, Henning A, et al. First clinical photon-counting detector CT system: technical evaluation. *Radiology* 2022;303:130–38 [CrossRef](#)
7. Leng S, Bruesewitz M, Tao S, et al. Photon-counting detector CT: system design and clinical applications of an emerging technology. *Radiographics* 2019;39:729–43 [CrossRef](#)
8. Willemink MJ, Persson M, Pourmorteza A, et al. Photon-counting CT: technical principles and clinical prospects. *Radiology* 2018; 289:293–312 [CrossRef](#)
9. Gutjahr R, Halaweish AF, Yu Z, et al. Human imaging with photon counting-based computed tomography at clinical dose levels: contrast-to-noise ratio and cadaver studies. *Invest Radiology* 2016; 51:421–29 [CrossRef](#)
10. Pourmorteza A, Symons R, Reich DS, et al. Photon-counting CT of the brain: in vivo human results and image-quality assessment. *AJNR Am J Neuroradiol* 2017;38:2257–63 [CrossRef](#)
11. Leng S, Rajendran K, Gong H, et al. 150-μm spatial resolution using photon-counting detector computed tomography technology: technical performance and first patient images. *Invest Radiology* 2018;53:655–62 [CrossRef](#)
12. Cao J, Bache S, Schwartz FR, et al. Pediatric applications of photon-counting detector CT. *AJR Am J Roentgenol* 2023;220:580–9 [CrossRef](#)
13. Hermans R, Boomgaert L, Cockmartin L, et al. Photon-counting CT allows better visualization of temporal bone structures in comparison with current generation multi-detector CT. *Insights Imaging* 2023;14:112 [CrossRef](#)
14. Rajendran K, Voss BA, Zhou W, et al. Dose reduction for sinus and temporal bone imaging using photon-counting detector CT with an additional tin filter. *Invest Radiology* 2020;55:91–100 [CrossRef](#)
15. Zhou W, Lane JI, Carlson ML, et al. Comparison of a photon-counting-detector CT with an energy-integrating-detector CT for temporal bone imaging: a cadaveric study. *AJNR Am J Neuroradiol* 2018;39:1733–38 [CrossRef](#)
16. Alzen G, Benz-Bohm G. Radiation protection in pediatric radiology. *Dtsch Arztebl Int* 2011;108:407–14 [CrossRef](#) [Medline](#)